Resolution in Diffraction-limited Imaging, a Singular Value Analysis

M. Bertero[a]; E. R. Pike[b]

[a] Istituto di Scienze Fisiche dell'Università and Istituto Nazionale di Fisica Nucleare, Genova, Italy. [b] Royal Radar and Signals Establishment, Malvern, England.

PLEASE SCROLL DOWN FOR ARTICLE

Resolution in diffraction-limited imaging, a singular value analysis

I. The case of coherent illumination

M. BERTERO

Istituto di Scienze Fisiche dell'Università and Istituto Nazionale di Fisica Nucleare, Genova, Italy

and E. R. PIKE

Royal Radar and Signals Establishment, Malvern, England

Abstract. The familiar theory of information transfer in imaging using the prolate spheroidal functions and their eigenvalue spectrum is extended to allow the object and image domains to differ. The appropriate theory becomes one of singular functions and singular values, and in this paper we give a description of coherent imaging in these terms. Super-resolution in the sense of improving on previous criteria in the presence of noise can then be achieved, particularly at very low Shannon numbers, using the physical continued image, and we give quantitative estimates of such improvements for the linear, square and circular pupil cases.

The theory is also shown to provide an efficient proof of the theorem that the number of degrees of freedom of a coherent isoplanatic imaging system is unaffected by phase aberrations in the pupil.

Applications of these results in microscopy are outlined, and a practical method of implementation is proposed based on a generalization of numerical inversion techniques developed recently in the field of laser scattering.

1. Introduction

Reconstruction of an object from a diffraction-limited image has been a central problem in optics, at least since the fundamental studies by Abbé and, more particularly, Lord Rayleigh. Rayleigh's well-known criterion has received continued application, most recently, for example, as a concept of the Shannon theory of information [1]. In this theory, which applies also to more general coherent inverse Fourier problems in communications, astronomy and radar, in which data are degraded by a noisy, linear, band-limited system, the number of Rayleigh resolution elements in an image is equated with its number of 'degrees of freedom', the Shannon number, by making use of the striking properties of the set of prolate spheroidal functions [2]. These oscillatory functions have the property of imaging themselves exactly, the only consequence of diffraction being to reduce the amplitude of transmission sharply if the number of oscillations across the object exceeds the Shannon number. In the case of incoherent 'illumination' a similar orthonormal set of functions exists, but numerical techniques are then necessary to obtain analogous results. In this paper we shall consider only the case of uniform coherent illumination. Calculations for the incoherent case are in progress, and we hope to present these in a later contribution. Here we present results for the cases of

circular and square pupils in two dimensions, but for the purposes of clarity carry through the written analysis using one dimension only. The methods are essentially identical.

In the one-dimensional case the general formulation of the problem in the absence of noise and with the magnification set equal to unity (without loss of generality) has the mathematical expression of inversion of the integral operator A defined by

$$(Af)(x) = \int_{-X/2}^{X/2} \frac{\sin [\Omega(x-y)]}{\pi(x-y)} f(y) \, dy, \quad |x| \leqslant X/2. \tag{1.1}$$

The function $(Af)(x)$ can be continued over the whole image space; then the Fourier transform of the analytic continuation of $(Af)(x)$ is zero outside $[-\Omega, \Omega]$.

We introduce the new variables $t = 2x/X$ and $c = X\Omega/2$, under which transformation equation (1.1) becomes

$$(Af)(t) = \int_{-1}^{1} \frac{\sin [c(t-s)]}{\pi(t-s)} f(s) \, ds, \quad |t| \leqslant 1. \tag{1.2}$$

The Shannon number is given by

$$S = \frac{2c}{\pi} = \frac{X\Omega}{\pi} \tag{1.3}$$

and the Rayleigh resolution distance by

$$R = \frac{X}{S} = \frac{\pi}{\Omega} = \frac{\pi X}{2c}. \tag{1.4}$$

The operator A maps the solution space $L^2(-1, 1)$ into the same data space (geometric image) and is self-adjoint, non-negative and compact; S is its trace. The equation $Af = 0$ has only the trivial solution $f = 0$ (uniqueness of the solution). The eigenfunctions of A are

$$u_k(t) = \lambda_k^{-1/2} \psi_k(c, t), \tag{1.5}$$

where $\psi_k(c, t)$ are the linear prolate spheroidal functions, and the eigenvalues of A are λ_k, that is to say

$$Au_k = \lambda_k u_k. \tag{1.6}$$

The u_k from a basis in $L^2(-1, 1)$, and may be regarded as elements of 'information' which retain their identity under the forward imaging transformation, save for a scaling in magnitude by the value λ_k. The larger λ_k, the more efficient is the transmission of the corresponding information element, but if the λ_ks are ordered in decreasing magnitude there will come a point at a sufficiently large value of k where the information is transmitted so weakly that it cannot be distinguished from experimental noise. The eigenvalue 'spectrum' λ_k has the property of decreasing extremely quickly from near unity to near zero at $k = S$. Even very small amounts of noise preclude the retrieval in practice of resolution in excess of that given by the Rayleigh criterion (super-resolution). Mathematically speaking, the problem of inversion is 'ill posed'; there exist images in the range of A such that their difference is arbitrarily small, even if they correspond to widely different objects. Such disparate solutions, therefore, become indistinguishable in the presence of noise. In

addition noise may displace the observed image out of the range of A, in which case no solution exists for the inversion problem, and no attempted physical inversion procedure will lead to unique results.

2. Analytic continuation, regularization and super-resolution

The ill-posedness described above has led in this and other similar problems to a great deal of mathematical research, dating back to Hadamard [3], on the existence, uniqueness and continuity of the solution on the data. Methods which have been proposed for super-resolution [4, 5] must be subject to the limitations of what is now a rather well-developed understanding of these problems [6]. For example, since the object is zero outside the interval $[-X/2, X/2]$, its Fourier transform is an entire analytic function; mathematically, therefore, analytic continuation in the frequency domain will allow restoration of unlimited detail [7], at least neglecting quantum-mechanical limitations on the measurement of the light field. The method fails in practice for the information-theoretic reasons given above. It should be noted that it does not fail for the reasons given by McCutchen [8] (uncritically quoted in an interesting tutorial paper by Pask [9]), who seems not to appreciate that analytic continuation makes use of only a finite range of frequency components.

A more useful approach to super-resolution recognizes that a set of possible objects can be constructed which are consistent with the data and a known noise level. A subset of this set is excluded to limit the effects of noise by imposing physical constraints. The method of regularization [10], for example, constrains the total radiated energy in the simplest case, or can limit higher derivatives of the object in more elaborate versions. The former is no more than sensible and could usefully restrict wild unphysical restoration; the latter could be even more selective in the presence of corroborating *a priori* information. Methods constraining intensities to be positive are also possible [11, 12]. In all cases, in the context of classical information theory, the achievement of resolution significantly beyond that pre-scribed by the Rayleigh criterion is, nevertheless, impractical [13, 15].

3. Reformulation of imaging theory as a singular value problem

As the object size reduces, the eigenfunctions and eigenvalues of the operator A introduced in equation (1.1) above, which arise when the range of x coincides with the range of integration, becomes less appropriate for a discussion of information content. This is because, although for normal objects much larger than the wavelength of light, the small diffraction spread outside the geometrical image contributes little to the problem, this is not so when we consider objects with sizes of only a few times R. The entire image, rather than the geometrically defined one, may be used for inversion and the two methods will be substantially different in the presence of noise. This possibility has been mentioned in the course of an eigenvalue analysis [13], but dismissed as having disadvantages. A complete discussion of this possibility requires the theory of singular function decomposition [16], and we give here a theory of imaging based on singular values and singular functions.

Let us call K the linear continuous integral operator from $F = L^2(-1, 1)$ to $G = L^2(-\infty, +\infty)$, which continues A over the whole image space, i.e.

$$(Kf)(t) = \int_{-1}^{1} \frac{\sin [c(t-s)]}{\pi(t-s)} f(s) \, ds, \quad -\infty < t + \infty. \tag{3.1}$$

Then, in the absence of noise, the solution of the inversion problem is equivalent to the solution of the integral equation

$$K\bar{f} = \bar{g}, \qquad (3.2)$$

where $\bar{f}$ is the 'true solution' in the space F of objects, and $\bar{g}$ a noiseless image in the range of K, $\bar{G}$. Hereafter the bar denotes the absence of noise. The closure of $\bar{G}$ is the space $\mathscr{B}$ of band-limited functions, i.e. the functions with Fourier transform (F.T.) zero outisde $[-c, c]$. Therefore any function in $\bar{G}$ is band-limited, but the converse is not always true: a band-limited function is not necessarily in $\bar{G}$, even if it is always a limit of functions of $\bar{G}$.

Using notation introduced by Slepian and Pollak [17], let us denote by B the projection operator over the subspace $\mathscr{B}$ of $L^2(-\infty, +\infty)$, i.e.

$$(Bg)(t) = \int_{-\infty}^{+\infty} \frac{\sin[c(t-s)]}{\pi(t-s)} g(s)\, ds = \frac{1}{2\pi} \int_{-c}^{-c} \hat{g}(\omega) \exp(i\omega t)\, d\omega; \qquad (3.3)$$

let us also denote by D the projection operator which restricts a function g of $L^2(-\infty, +\infty)$ to the interval $[-1, 1]$:

$$(Dg)(t) = \begin{cases} g(t), & |t| \leqslant 1 \\ 0, & |t| > 1. \end{cases} \qquad (3.4)$$

If $\bar{g}$ is a noiseless image, then $B\bar{g} = \bar{g}$, while $D\bar{g}$ is the restriction of $\bar{g}$ to the geometrical image region.

Consider the operator K^*, the adjoint of the operator K. Since the kernel of K is real, we have $K^* = K^T$. It is easily verified that $K^T = DB$, i.e.

$$(K^T g)(t) = \int_{-\infty}^{+\infty} \frac{\sin[c(t-s)]}{\pi(t-s)} g(s)\, ds, \quad |t| \leqslant 1. \qquad (3.5)$$

Therefore the null space of K^T is the subspace of the L^2 functions whose F.T. is zero over $[-c, c]$ or, in other words, the orthogonal complement of the space of band-limited functions. From these properties, and equations (1.2) and (3.1), it follows that $K^T K = DBK = DK = A$. The orthonormal system of the eigenfunctions of $K^T K$ is given by equation (1.5) as

$$K^T K u_k = \lambda_k u_k. \qquad (3.6)$$

If we introduce the functions

$$v_k(t) = \psi_k(c, t), \quad -\infty < t < +\infty, \qquad (3.7)$$

which are an orthonormal system in $\mathscr{B}$, then, from the fundamental properties of the ψ_k,

$$\int_{-1}^{1} \frac{\sin[c(t-s)]}{\pi(t-s)} \psi_k(c, s)\, ds = \lambda_k \psi_k(c, t), \qquad (3.8)$$

$$\int_{-\infty}^{+\infty} \frac{\sin[c(t-s)]}{\pi(t-s)} \psi_k(c, s)\, ds = \psi_k(c, t), \qquad (3.9)$$

we have

$$K u_k = \sqrt{\lambda_k}\, v_k, \qquad (3.10)$$

$$K^T v_k = \sqrt{\lambda_k}\, u_k. \qquad (3.11)$$

Using expansions in terms of the singular functions u_k and v_k, and singular values $\lambda_k^{1/2}$, one can easily solve the integral equation (3.2). Indeed, the singular functions u_k form a complete set in F, while the singular functions v_k form a complete set in $\mathscr{B}$. Then any noiseless image $\bar{g}$ can be expanded as

$$\bar{g}(t) = \sum_{k=0}^{+\infty} \bar{g}_k v_k(t), \qquad (3.12)$$

where

$$\bar{g}_k = \int_{-\infty}^{+\infty} \bar{g}(t) v_k(t)\, dt. \qquad (3.13)$$

As follows from equation (3.10), the solution of equation (3.2) corresponding to $\bar{g}$ is

$$\bar{f}(t) = \sum_{k=0}^{+\infty} \frac{\bar{g}_k}{\sqrt{\lambda_k}} u_k(t). \qquad (3.14)$$

We may compare this result with the result of the eigenfunction method. In the latter case, the noiseless data are the restriction of $\bar{g}$ to the geometrical region, i.e. $D\bar{g}$. From the eigenfunction expansion

$$(D\bar{g})(t) = \sum_{k=0}^{+\infty} \bar{g}_k' u_k(t), \qquad (3.15)$$

where

$$\bar{g}_k' = \int_{-1}^{1} \bar{g}(t) u_k(t)\, dt, \qquad (3.16)$$

we find that the solution of the integral equation $A\bar{f} = D\bar{g}$ is

$$\bar{f}(t) = \sum_{k=0}^{+\infty} \frac{\bar{g}_k'}{\lambda_k} u_k(t). \qquad (3.17)$$

Now, equation (3.10) implies that the following relation holds:

$$\begin{aligned}
\bar{g}_k &= \int_{-\infty}^{+\infty} \bar{g}(t) v_k(t)\, dt = \frac{1}{\sqrt{\lambda_k}} \int_{-\infty}^{+\infty} \bar{g}(t)(Ku_k)(t)\, dt \\
&= \frac{1}{\sqrt{\lambda_k}} \int_{-1}^{1} u_k(s) \left(\int_{-\infty}^{+\infty} \frac{\sin[c(s-t)]}{\pi(s-t)} \bar{g}(t)\, dt \right) ds \\
&= \frac{1}{\sqrt{\lambda_k}} \int_{-1}^{1} \bar{g}(s) u_k(s)\, ds \\
&= \frac{1}{\sqrt{\lambda_k}} \bar{g}_k', \qquad (3.18)
\end{aligned}$$

where the property $B\bar{g} = \bar{g}$ has been used. As a consequence, the solutions (3.14) and (3.17) coincide.

We see therefore that an inversion of a noiseless image can be performed using either the singular-value analysis (equations (3.13) and (3.14)) or the eigenfunction analysis (equations (3.16) and (3.17)). In the former case the complete diffracted image is used, while in the latter only those points lying within the geometric image

are required. This equivalence, however does not extend to the real case where *out-of band noise* is present. In this case the eigenfunction inversion requires, one might say, the solution of two ill-posed problems: the first, to extrapolate the image outside $[-1, 1]$ [18] and the second, to solve the singular-value problem. By omitting the first stage we will be able to improve the optical resolution which can be achieved in inversion, particularly at low Shannon numbers.

4.   The effect of noise on inversion

Since the u_ks form a basis in $F = L^2(-1, 1)$, any object in that class can be represented by the expansion

$$\bar{f}(t) = \sum_{k=0}^{+\infty} \bar{a}_k u_k(t), \quad |t| \leqslant 1. \tag{4.1}$$

The coefficients $\bar{a}_k$ are reconstructed by the unconstrained inversion procedures described above, either as

$$\bar{a}_k = \frac{1}{\sqrt{\lambda_k}} \int_{-\infty}^{+\infty} \bar{g}(t) v_k(t) \, dt \tag{4.2}$$

if the singular functions method is chosen, or as

$$\bar{a}_k = \frac{1}{\lambda_k} \int_{-1}^{1} \bar{g}(t) u_k(t) \, dt \tag{4.3}$$

when the eigenfunction method is used. The two methods are formally equivalent when $\bar{g} \in \bar{G}$ and, more generally, for images corrupted by band-limited noise. The difference between the two methods appears in their response to out-of-band noise.

Let us take as the real image of $\bar{f}$

$$g(t) = \bar{g}(t) + n(t), \quad -\infty < t < +\infty, \tag{4.4}$$

where $n(t)$ is the image noise, presumed additive. Using equations (3.12), (3.13) and (4.2), we have

$$\bar{g}(t) = \sum_{k=0}^{+\infty} \sqrt{\lambda_k} \bar{a}_k v_k(t) \tag{4.5}$$

and we may resolve $n(t)$ into in-band and out-of-band components

$$n(t) = \sum_{k=0}^{+\infty} b_k v_k(t) + \frac{1}{2\pi} \int_{|\omega| > c} \hat{n}(\omega) \exp(it\omega) \, d\omega, \tag{4.6}$$

where

$$b_k = \int_{-\infty}^{+\infty} n(t) v_k(t) \, dt. \tag{4.7}$$

Now, the effect of noise on the coefficients of the reconstructed object in the singular-value method is given by

$$a_k^{(S)} = \frac{1}{\sqrt{\lambda_k}} \int_{-\infty}^{+\infty} g(t) v_k(t) \, dt = \bar{a}_k + \frac{b_k}{\sqrt{\lambda_k}}, \tag{4.8}$$

as follows from equations (4.4), (4.5) and (4.6). No contributions arise from the out-of-band noise since it is orthogonal to the linear prolate spheroidal functions. On the

other hand, in the eigenfunction method, the effect of noise on the reconstructed coefficients is given by

$$a_k^{(E)} = \frac{1}{\lambda_k} \int_{-1}^{1} g(t) u_k(t) \, dt = \bar{a}_k + \frac{b_k}{\sqrt{\lambda_k}} + \frac{c_k}{\lambda_k}, \qquad (4.9)$$

where

$$c_k = \frac{1}{2\pi} \int_{|\omega| > c} \hat{n}(\omega) \left(\int_{-1}^{1} u_k(t) \exp(i\omega t) \, dt \right) d\omega$$

$$= \frac{(-1)^k}{\sqrt{(2\pi c)}} \int_{|\omega| > c} \hat{n}(\omega) \psi_k \left(c, \frac{\omega}{c} \right) d\omega. \qquad (4.10)$$

In deriving equation (4.9), we have again used equations (4.4), (4.5) and (4.6); also, in equation (4.10) the following property of the linear prolate spheroidal functions has been used [2]:

$$\int_{-1}^{1} \psi_k(c, t) \exp(i\omega t) \, dt = (-1)^{k/2} \left(\frac{2\pi \lambda_k}{c} \right)^{1/2} \psi_k \left(c, \frac{\omega}{c} \right). \qquad (4.11)$$

Equations (4.8) and (4.9) coincide in the case of band-limited noise, i.e. $\hat{n}(\omega) = 0$ for $|\omega| > c$, while in the presence of out-of-band noise equation (4.9) contains an additional term.

In passing we should note that it has been suggested that in the eigenfunction method a smoothing should be performed on the data to reduce the effect of noise on inversion, and calculations of the expected effects of such smoothing have been made [13]. That this is not possible without degrading the reconstructed image is easily shown by the following argument. Let L be a linear smoothing operator to be applied to the data. Then we require that

$$LD(\bar{g} + n) = D\bar{g} + LDn; \qquad (4.12)$$

the smoothed LDn would then be expected to have a less harmful effect on the inversion procedure. However, $D\bar{g}$ is dense in $L^2(-1, 1)$ and hence, since

$$LD\bar{g} = D\bar{g}, \qquad (4.13)$$

we must have

$$LDg = LDg, \qquad (4.14)$$

where g is an arbitrary L^2 function. The only operator which satisfies equation (4.14) is the identity, and hence the operation proposed is impossible. We will, however, be able to obtain similar beneficial effects without distortion of the object using the singular-value method.

In order to estimate the various terms in equations (4.8) and (4.9), let us assume that the object $\bar{f}(t)$ is from a white-noise process with power spectrum E^2,

$$\langle f^*(t) \bar{f}(t') \rangle = E^2 \delta(t - t'), \qquad (4.15)$$

and that the image noise is also white with power spectrum

$$\langle n^*(t) n(t') \rangle = \varepsilon^2 \delta(t - t'), \qquad (4.16)$$

which implies that

$$\langle \hat{n}^*(\omega) n(\omega') \rangle = 2\pi \varepsilon^2 \delta(\omega - \omega'). \qquad (4.17)$$

Let us further assume that the two processes are uncorrelated,

$$\langle \bar{f}^*(t)n(t') \rangle = 0, \tag{4.18}$$

then from equations (4.7) and (4.16) we obtain

$$\langle |b_k|^2 \rangle = \varepsilon^2, \tag{4.19}$$

and from equations (4.10) and (4.17) we obtain

$$\langle |c_k|^2 \rangle = \varepsilon^2(1 - \lambda_k). \tag{4.20}$$

As a consequence, the variances of the reconstructed coefficients in the singular-value method are given by

$$\langle |a_k^{(S)}|^2 \rangle = E^2 + \frac{\varepsilon^2}{\lambda_k}, \tag{4.21}$$

while in the eigenfunction method they are given by

$$\langle |a^{(E)}|^2 \rangle = E^2 + \frac{\varepsilon^2}{\lambda_k} + \frac{\varepsilon^2(1 - \lambda_k)}{\lambda_k^2} = E^2 + \frac{\varepsilon^2}{\lambda_k^2}. \tag{4.22}$$

Therefore the variance of the second term in equation (4.9) is of the order of λ_k^{-1} as $k \rightarrow +\infty$, while the variance of the third term is of the order of λ_k^{-2}. As k exceeds the Shannon number and λ_k tends to zero, the 'amplification' of the out-of-band noise is much greater than the amplification of the in-band noise, and thus the instability of the eigenfunction method is much more severe than when using the singular functions.

5. Resolution limits

The previous analysis demonstrates that the suppression of the out-of-band noise provided by the projection on singular functions must produce an improvement in the inversion procedure. We can estimate this improvement as follows.

Consider first the singular function method. Then from equation (4.17) it follows that, in the inversion procedure, we can estimate only those components such that the variance E^2 of the object (signal) is greater than the variance in the reconstruction of the noise, $\varepsilon^2 \lambda_k^{-1}$, i.e. those components for which

$$\lambda_k \geqslant (\varepsilon/E)^2. \tag{5.1}$$

Analogously, as regards the eigenfunction method, from equation (4.22) it is possible to estimate only those components of the object such that

$$\lambda_k \geqslant \varepsilon/E. \tag{5.2}$$

Since the eigenvalues are ordered in a decreasing sequence, then condition (5.1) is satisfied for $k \leqslant N_S$, and condition (5.2) is satisfied for $k \leqslant N_E$. Therefore the first method allows the determination of $M_S = N_S + 1$ components of the object, while the second method allows the determination of $M_E = N_E + 1$ components. When $\varepsilon/E < 1$, we have always $M_S \geqslant M_E$, and hence we always obtain an improvement by using the singular-value method.

Now, when $M = N + 1$ terms are determined in the expansion of the object, a reasonable measure of the resolution achieved is the average distance between the zeros of $u_N(t)$. Using again the variable $x = Xt/2$ (X is the size of the object) and

remarking that $u_N(2x/X)$ has exactly N zeros in $[-X/2, X/2]$, the above measure of resolution is given by

$$D = X/(N+1) = (S/M)R. \qquad (5.3)$$

The quantity M is an 'effective number of degrees of freedom', and is a function of the 'signal-to-noise ratio' E/ε. Therefore, from equation (5.3) one can derive the ratio R/D, the number of resolution elements restored within the Rayleigh distance, as a function of the signal-to-noise ratio and of the Shannon number.

The number of components $M_S = N_S + 1$ and the corresponding number of resolution elements R/D_S achieved by the singular-value method can be easily computed for various values of the Shannon number and the signal-to-noise ratio E/ε. We use equation (5.1) and values of λ_k given in [2]. Some results are given in table 1, using a linear interpolation between the eigenvalues. A graphical representation is shown in figure 1.
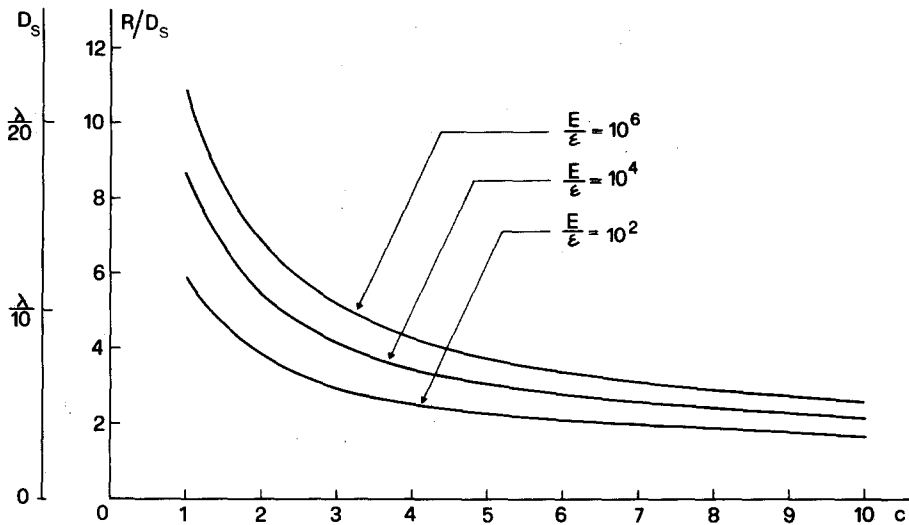

Figure 1. Super-resolution gain using singular-value method on complete image for various values of signal-to-noise ratio, E/ε. Linear case. The scale on the extreme left shows the linear resolution possible with $R = \lambda/2$.

6. The effect of aberrations

It has been already pointed out that, when the entire image is used, the effective number of degrees of freedom is independent of aberrations and equal to the number of degrees of freedom in the aberration-free case [19]. We show how the singular-function expansions provide a very beautiful and simple analysis of this problem.

When the image is isoplanatic but suffers from aberrations, one can take into account their effect by multiplying the pupil function of the unaberrated optical system by a pure phase factor [20]. Then equation (3.1) has to be replaced by

$$(K_\alpha f)(t) = \int_{-1}^{1} S_\alpha(t-s)f(s)\,ds, \quad -\infty < t < +\infty, \qquad (6.1)$$

Table 1. Number of components, M_S, and corresponding number of resolution elements within the Rayleigh distance R/D_S, restored by the singular value method, as a function of 'signal-to-noise ratio', E/ε; linear case.

E/ε	$c=1$		$c=2$		$c=3$		$c=4$		$c=5$		$c=6$		$c=7$		$c=8$		$c=9$		$c=10$	
	M_S	R/D_S	M_S	R/D_S	M_S	R/D_S	M_S	R/D_S	M_S	R/D_S	M_S	R/D_S	M_S	R/D_S	M_S	R/D_S	M_S	R/D_S	M_S	R/D_S
10^2	3·78	5·93	4·81	3·77	5·74	3·01	6·59	2·59	7·34	2·31	7·99	2·09	8·86	1·99	9·66	1·90	10·36	1·81	10·98	1·72
10^4	5·51	8·65	6·84	5·37	7·90	4·14	8·91	3·50	9·87	3·10	10·80	2·82	11·69	2·62	12·51	2·46	13·25	2·31	13·97	2·19
10^6	6·94	10·90	8·67	6·81	9·88	5·17	10·95	4·30	11·95	3·75	12·97	3·40	13·95	3·13	14·91	2·93	15·84	2·76	16·75	2·63

where

$$S_\alpha(t) = \frac{1}{2\pi} \int_{-c}^{c} \exp\left[i\alpha(\omega) + i\omega t\right] d\omega. \tag{6.2}$$

K_α is a linear compact operator from $L^2(-1, 1)$ into $L^2(-\infty, +\infty)$ and its range is dense in $\mathscr{B}$, so that $BK_\alpha = K_\alpha$. Then the adjoint operator K_α^* is given by

$$(K_\alpha^* g)(t) = \int_{-\infty}^{+\infty} S_\alpha^*(s - t)g(s)\, ds, \quad |t| \leqslant 1, \tag{6.3}$$

where $S_\alpha^*(t)$ denotes the complex conjugate of $S_\alpha(t)$. From the relation $BK_\alpha = K_\alpha$, it follows that $K_\alpha^* = K_\alpha^* B$, and therefore the null space of K_α^* is the orthogonal complement of $\mathscr{B}$. It then follows that

$$(K_\alpha^* K_\alpha f)(t) = \int_{-1}^{1} H(t - s)f(s)\, ds, \quad |t| \leqslant 1 \tag{6.4}$$

where

$$H(t) = \int_{-\infty}^{+\infty} S_\alpha(s - t)S_\alpha^*(s)\, ds \quad \text{(Parseval equality)} \tag{6.5}$$

$$= \frac{1}{2\pi} \int_{-c}^{c} \exp\left[i\alpha(\omega) - i\omega t\right] \exp\left[-i\alpha(\omega)\right] d\omega = \frac{\sin(ct)}{\pi t}.$$

Therefore the singular values of the operator K_α are always given by the square roots of the eigenvalues of the prolate spheroidal functions and the singular functions $u_k(t)$ are always given by equation (1.5).

If we denote by $v_{k,\alpha}(t)$ the eigenfunctions of the operator $K_\alpha K_\alpha^*$, then we have the analogues of equations (3.10), (3.11), i.e.

$$K_\alpha u_k = \sqrt{\lambda_k}\, v_{k,\alpha}, \tag{6.6}$$

$$K_\alpha^* v_{k,\alpha} = \sqrt{\lambda_k}\, u_k, \tag{6.7}$$

where

$$v_{k,\alpha}(t) = \frac{1}{\sqrt{\lambda_k}} \int_{-1}^{1} S_\alpha(t - s)u_k(s)\, ds = \int_{-\infty}^{+\infty} S_\alpha(t - s)\psi_k(c, s)\, ds \tag{6.8}$$

(in the last equation the band-limiting of $S_\alpha(t)$ has been used). The singular functions $v_{k,\alpha}(t)$ coincide with the functions $G_k(t)$ introduced in [19]. Since, as we have already remarked, the null space of K_α^* is just the orthogonal complement of $\mathscr{B}$, it follows that the $v_{k,\alpha}$ form a complete orthonormal basis in $\mathscr{B}$.

Using these properties, the analysis developed in §§ 3–5 can be immediately extended to the case of aberrated images, at least when the entire image is supposed to be known. However, it is not easy to make a comparison with the case where the image is given only in the geometrical region. Indeed, in this case, the appropriate operator is

$$(A_\alpha f)(t) = \int_{-1}^{1} S_\alpha(t - s)f(s)\, ds, \quad |t| \leqslant 1, \tag{6.9}$$

which is not self-adjoint. It is only in certain cases of coherent imaging that simple relations hold between the singular functions and singular values and the prolate spheroidal functions and their eigenvalues. For equation (6.9), and also for the incoherent imaging case, such relations, unfortunately, do not exist.

7. The two-dimensional case

We outline here the extension of the previous results to the case of two-dimensional objects in coherent illumination. We consider only the singular-function method and aberration-free images.

If we denote by $\mathbf{x} = \{x_1, x_2\}$ a point in the object plane, and if the complex amplitude of the object $f(\mathbf{x})$ is different from zero only on the bounded domain $\mathscr{D}$, then the noise-free image $\bar{g}(\mathbf{x})$ is given by

$$(Kf)(\mathbf{x}) = \iint_{\mathscr{D}} S(\mathbf{x} - \mathbf{y}) f(\mathbf{y}) \, d\mathbf{y}, \qquad (7.1)$$

where

$$S(\mathbf{x}) = \frac{1}{(2\pi)^2} \iint_{\mathscr{A}} \exp\left[i(\mathbf{x}, \omega)\right] d\omega, \qquad (7.2)$$

$\mathscr{A}$ being the bounded domain in Fourier space corresponding to the frequencies which are transmitted by the instrument. The operator K is a compact operator from $L^2(\mathscr{D})$ into $L^2(\mathbb{R}^2)$ and the adjoint operator K^* is given by

$$(K^* g)(\mathbf{x}) = \iint \int_{-\infty}^{+\infty} S^*(\mathbf{y} - \mathbf{x}) g(\mathbf{y}) \, d\mathbf{y} = \iint \int_{-\infty}^{+\infty} S(\mathbf{x} - \mathbf{y}) g(\mathbf{y}) \, d\mathbf{y}, \quad \mathbf{x} \in \mathscr{D}. \qquad (7.3)$$

Using the relation

$$\iint \int_{-\infty}^{+\infty} S(\mathbf{x} - \mathbf{y}) S(\mathbf{y}) \, d\mathbf{y} = S(\mathbf{x}), \qquad (7.4)$$

we obtain

$$(K^* K f)(\mathbf{x}) = \iint_{\mathscr{D}} S(\mathbf{x} - \mathbf{y}) f(\mathbf{y}) \, d\mathbf{y}, \quad \mathbf{x} \in \mathscr{D}. \qquad (7.5)$$

The operator $K^* K$ is a self-adjoint, non-negative, compact operator in $L^2(\mathscr{D})$; its eigenfunctions are the generalized prolate spheroidal functions $\psi_k(\mathbf{x})$ introduced by Slepian [21]. If we denote by λ_k the corresponding eigenvalues, then the $\psi_k(\mathbf{x})$ are normalized in such a way that

$$\iint_{\mathscr{D}} \psi_k(\mathbf{x}) \psi_j^*(\mathbf{x}) \, dx = \lambda_k \delta_{kj}, \qquad (7.6)$$

and they have the double orthogonality property

$$\iint \int_{-\infty}^{+\infty} \psi_k(\mathbf{x}) \psi_j^*(\mathbf{x}) \, d\mathbf{x} = \delta_{kj}. \qquad (7.7)$$

Therefore, introducing the functions

$$u_k(\mathbf{x}) = \frac{1}{\sqrt{\lambda_k}} \psi_k(\mathbf{x}), \quad v_k(\mathbf{x}) = \psi_k(\mathbf{x}), \qquad (7.8)$$

the following relations hold:

$$K u_k = \sqrt{\lambda_k} v_k, \quad K^* v_k = \sqrt{\lambda_k} u_k. \qquad (7.9)$$

Since the set of the u_k functions forms an orthonormal basis in $L^2(\mathscr{D})$, while the set of the v_k functions forms an orthonormal basis in the subspace of band-limited functions whose F.T. has a support contained in $\mathscr{A}$, the analysis carried out in §3 can

be immediately extended to this more general case. We consider now two particular cases.

Square object and square pupil.

Let us assume that the domain of the object is $\mathscr{D} = [-X/2, X/2] \times [-X/2, X/2]$, and that the 'pupil' of the instrument is $a = [-\Omega, \Omega] \times [-\Omega, \Omega]$. Then the point-spread function (6.2) is

$$S(x) = \frac{\sin(\Omega x_1)}{\pi x_1} \frac{\sin(\Omega x_2)}{\pi x_2} . \qquad (7.10)$$

Introducing again the variables $\mathbf{t} = 2\mathbf{x}/X$ and $c = X\Omega/2$, the singular functions and singular values of the operator, (6.1) and (6.10), can be expressed in terms of the singular function and singular values of the operator (3.1):

$$\left. \begin{aligned} u_{i,k}(\mathbf{t}) &= u_i(t_1)u_k(t_2), \\ v_{i,k}(\mathbf{t}) &= v_i(t_1)v_k(t_2) \\ \sqrt{(\lambda_{i,k})} &= \sqrt{(\lambda_i \lambda_k)}. \end{aligned} \right\} \qquad (7.11)$$

In particular, the singular values can be easily computed using the eigenvalues of the linear prolate spheroidal functions.

We shall denote again by M_S the number of components satisfying the condition

$$\lambda_{i,k} = \lambda_i \lambda_k \geqslant (\varepsilon/E)^2; \qquad (7.12)$$

the area of a resolution element contained in $\mathscr{D}$ is then

$$D_S^2 = \frac{X^2}{M_S} \qquad (7.13)$$

and the number of resolution elements contained in the Rayleigh area $R^2 = (\pi/\Omega)^2$ is

$$\frac{R^2}{D_S^2} = \left(\frac{R^2}{X^2} \right) M_S = \left(\frac{\pi}{2c} \right)^2 M_S. \qquad (7.14)$$

Results are given in table 2 and presented graphically in figure 2.

Circular object and circular pupil

We assume that the domain $\mathscr{D}$ of the object is a circle of radius $X/2$ and that the domain of transmitted frequencies is a circle of radius Ω. Then the point-spread function (6.2) is

$$S(\mathbf{x}) = \frac{\Omega}{2\pi} \frac{J_1(\Omega|\mathbf{x}|)}{|\mathbf{x}|} , \qquad (7.15)$$

in which case the Rayleigh distance is

$$R = 1 \cdot 22 \frac{\pi}{\Omega} . \qquad (7.16)$$

Table 2. Number of components, M_S, and corresponding number of resolution elements within the Rayleigh area, $(R/D_S)^2$, restored by the singular value method, as a function of 'signal-to-noise ratio', E/ϵ; square pupil case.

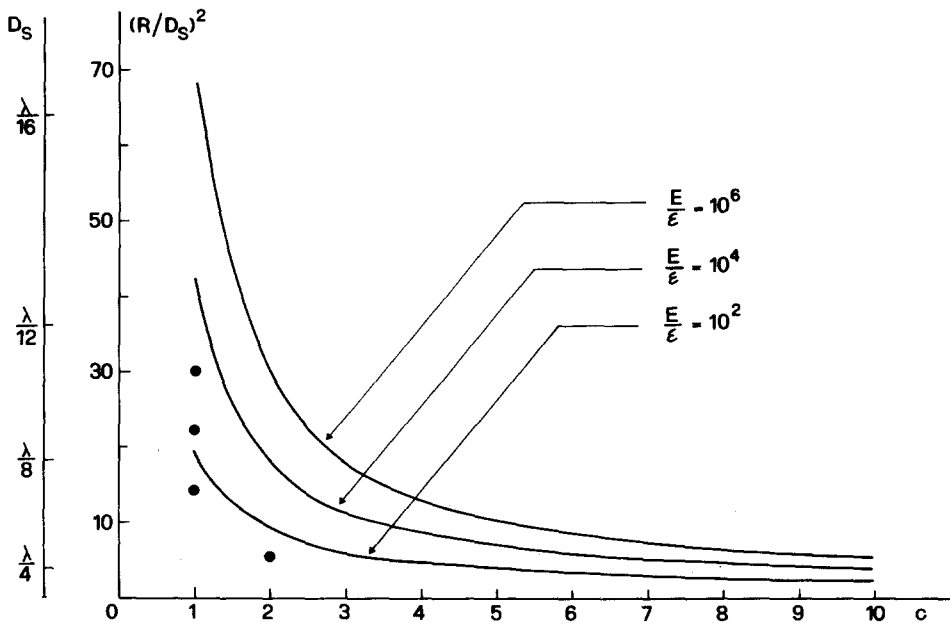| E/ϵ	$c=1$		$c=2$		$c=3$		$c=4$		$c=5$		$c=6$		$c=7$		$c=8$		$c=9$		$c=10$	
	M_S	$(R/D_S)^2$	M_S	$(R/D_S)^2$	M_S	$(R/D_S)^2$	M_S	$(R/D_S)^2$	M_S	$(R/D_S)^2$	M_S	$(R/D_S)^2$	M_S	$(R/D_S)^2$	M_S	$(R/D_S)^2$	M_S	$(R/D_S)^2$	M_S	$(R/D_S)^2$
10^2	7·86	19·4	14·5	8·94	22·5	6·17	30·8	4·74	42·1	4·15	48·9	3·35	61·1	3·07	75·3	2·90	91·0	2·77	98·5	2·42
10^4	17·20	42·5	29·5	18·10	41·4	11·30	55·2	8·50	70·8	6·98	86·9	5·95	105·4	5·30	122·9	4·73	145·7	4·43	155·7	3·83
10^6	27·60	68·0	47·7	29·40	65·2	17·90	83·7	12·90	102·0	10·10	124·5	8·53	146·7	7·38	168·5	6·49	195·6	5·95	220·2	5 42

Figure 2.   Super-resolution gain using singular-value method on complete image for various values of signal-to-noise ratio, E/ε. Two-dimensional case. The lines are for the square pupil, and the circles give values for the circular pupil for $E/\varepsilon = 10^2$, 10^3 and 10^4 at $c = 1$ and 10^2 at $c = 2$. The scale on the extreme left shows the linear resolution possible with $R = \lambda/2$.

Introducing again the variables $\mathbf{t} = 2\mathbf{x}/X$ and $c = X\Omega/2$, and using polar coordinates $t = |\mathbf{t}|, \phi$, the singular functions of the operator, (6.1) and (6.15), are given by

$$u_{n,m}(\mathbf{t}) = (2\pi t \lambda_{n,m})^{-1/2} \varphi_{n,m}(c, t) \exp(in\phi) \tag{7.17}$$

$$v_{n,m}(\mathbf{t}) = (2\pi t)^{-1/2} \varphi_{n,m}(c, t) \exp(in\phi) \tag{7.18}$$

where the $\varphi_{n,m}(t)$ are the circular prolate functions, solutions of the eigenvalue problem

$$\int_0^1 \sqrt{(ts)} K_n(c; t, s) \varphi_{n,m}(c, s)\, ds = \lambda_{n,m} \varphi_{n,m}(c, t), \tag{7.19}$$

$$K_n(c; t, s) = \int_0^c \omega J_n(\omega t) J_n(\omega s)\, d\omega, \tag{7.20}$$

and satisfying the orthogonality conditions

$$\int_0^1 \varphi_{n,m}(c, t) \varphi_{n,l}(c, t)\, dt = \lambda_{n,m} \delta_{lm}, \tag{7.21}$$

$$\int_0^{+\infty} \varphi_{n,m}(c, t) \varphi_{n,l}(c, t)\, dt = \delta_{lm}. \tag{7.22}$$

The singular values of the operator, (6.1) and (6.15), are given again by $\sqrt{\lambda_{n,m}}$, and one can compute the number M_S of eigenvalues satisfying the condition $\lambda_{n,m} \geqslant (\varepsilon/E)^2$.

The area of a resolution element contained in $\mathscr{D}$ is then given by

$$\pi\left(\frac{D_S}{2}\right)^2 = \pi\left(\frac{X}{2}\right)^2 \frac{1}{M_S}, \qquad (7.23)$$

and therefore the number of resolution elements contained in the area of a Rayleigh element is

$$\frac{R^2}{D_S^2} = \left(\frac{R}{X}\right)^2 M_S = \left(\frac{1\cdot22\pi}{2c}\right)^2 M_S. \qquad (7.24)$$

Some results are given in table 3; unfortunately in this case not many values of $\lambda_{n,m}$ are at our disposal. These values are shown also in figure 2.

Table 3. Number of components, M_S, and corresponding number of resolution elements within the area of a Rayleigh element, $(R/D_S)^2$, restored by the singular value method, as a function of 'signal-to-noise ratio', E/ε; circular pupil case.

E/ε	$c=1$		$c=2$	
	M_S	$(R/D_S)^2$	M_S	$(R/D_S)^2$
10^2	4·00	14·7	>6	>5·51
10^3	5·97	21·9	—	—
10^4	~8	~30	—	—

8. Application to microscopy

The results of the above analysis clearly indicate that quite considerable improvements in the performance of imaging systems can be expected if the theory can be put into practice. The optical microscope immediately comes to mind, and one might expect that developments of existing scanning microscopes [22], using laser illumination to achieve low Shannon numbers and high E/ε, values would provide systems suitable for application of these singular-value techniques. Unfortunately, however, the ultimate performance of a well-designed microscope of this type should be limited by photon noise in the image, and this analysis, which took only additive noise into account, would not then strictly apply. Further work is required, therefore, along the lines of existing photon-statistics literature [23], to investigate this case quantitatively, but one might proceed to construct an instrument in the hope that, qualitatively, similar improvements may be obtained. The incoherent case with additive image noise, which we shall discuss in a later paper, will likewise have a similar limitation when applied to optical systems. It is possible, however, that the present analysis has a direct application to scanning acoustic microscopes and other lower-frequency imaging systems and for these and for possible optical realization we therefore give an indication of how such a system could be constructed in practice.

Unfortunately also in the optical case, for an exact application of the theory the complex amplitudes of the image must be derived from the intensities. If the object may be assumed to be real this may not be too difficult since the problem, in the absence of noise, has a unique solution. Otherwise the recently proposed method of Walker [24] may be considered or, alternatively, a reference beam method may be necessary. For biological objects fortunately, the zero-order diffraction removes this

problem automatically since no phase ambiguity will exist for mainly transparent specimens.

We take as a model recent work [25, 26] in the inversion of light-scattering data, in which successful inversions of the Laplace and other integral transforms based on similar information-theoretic considerations have been accomplished by simple numerical sampling techniques.

We consider the discrete linear problem

$$\sum_n K^{(D)}_{mn} f_n = g_m \tag{8.1}$$

where $K^{(D)}$ is an $M \times N$ matrix, $M \geqslant N$,

$$K^{(D)}_{mn} = K(t_m, s_n) w_n, \tag{8.2}$$

where the weights w_n depend on the form of quadrature and $\mathbf{f}$ and $\mathbf{g}$ are vectors $\{f(s_n)\}$ and $\{g(t_m)\}$ in N- and M-dimensional euclidean spaces F_N and G_M respectively. When $M > N$, a solution of equation (8.1) usually does not exist, and then one considers the solution of the least-squares problem associated with (8.1):

$$\|K^{(D)}\mathbf{f} - \mathbf{g}\|_M = \text{minimum}, \tag{8.3}$$

i.e.

$$\sum_n (K^{(D)T} K^{(D)})_{mn} f_n = (K^{(D)T} g)_m. \tag{8.4}$$

It has been found in practice, numerically, in the light-scattering work quoted above and, explicitly, in work which we have in preparation, that the condition number of this sampled problem (that is to say the ratio of the largest to the smallest singular value of $K^{(D)}$), is well approximated by the ratio of the singular values of the first and Nth singular functions of the continuous transformation K, provided that the dispersion of the samples and the weights w_n are chosen to correspond to the positions of the nodes and the integrated amplitudes between nodes, respectively, of the Nth singular function of the continuous transform. The suppression of out-of-band noise can also be shown to occur by the following argument.

Let a basis for $K^T g$ in F_N be given by a complete set of functions $\varphi_m(t)$ so that

$$(K^T g)(t) = \sum_{m=1}^N c_m \varphi_m(t); \tag{8.5}$$

then the vector components of $K^T g$ are

$$c_m = (K^T g)_m = \int_{-\infty}^{+\infty} (K\varphi_m)(t) g(t) \, dt. \tag{8.6}$$

But, since $(K\varphi_m)(t)$ is band-limited,

$$(K^T g)_m = \int_{-\infty}^{+\infty} (K\varphi_m)(t)(Bg)(t) \, dt \tag{8.7}$$

and the integral suppresses the out-of-band noise in g. A quadrature by trapezoidal rule of equation (8.6) gives the approximation

$$(K^T g)_m = \sum_{j=1}^N (K\varphi_m)(t_j) g(t_j), \tag{8.8}$$

which is the exact value (apart from end-effects) of the integral of a band-limited function with the summand values at the sample points. If, therefore, using this quadrature, we take our samples in G_M at the Nyquist rate of the integrand, i.e. the sum of that of the spatial noise present in the image and that of $(K\varphi_m)(t)$, we will obtain an exact elimination by projection of those components of noise above the transmission band limit. In so far as this sampling rate is not achieved, some out-of-band noise will be present in the reconstruction, and the full advantage of the singular-value method will not be obtained.

An approximate numerical sampling technique for the imaging kernel discussed in this paper would thus be furnished simply by equally spaced (in one or two dimensions) detectors integrating over each sampling element. The values of $(K\varphi_m)(t_j)$ can be stored for any choice of object basis functions φ_m to compute the integral (8.6). If desired, these functions may conveniently be chosen as a set of equally spaced δ-functions, as in the exponential sampling method of Ostrowski *et al.* [26], in which case

$$(K\varphi_m)(t) = \frac{\sin c(t-t_m)}{\pi(t-t_m)}. \tag{8.9}$$

The $N \times N$ matrix

$$(K^{\mathrm{T}}K)_{mn} = \int_{-\infty}^{+\infty} (K\varphi_m)(t)(K\varphi_n)(t)\, dt \tag{8.10}$$

can be calculated by use of the sampling theorem using only values at the sampling points t_j of the image

$$(K^{\mathrm{T}}K)_{mn} = \sum_j (K\varphi_m)(t_j)(K\varphi_n)(t_j), \tag{8.11}$$

and finally equation (8.4) must be inverted using a stable numerical inversion programme. It should be noted that the dimension of the (square) matrix $K^{(\mathrm{D})\mathrm{T}}K^{(\mathrm{D})}$ to be inverted will normally be much less than the number of sample points in the image. The computations may, alternatively, be performed using a numerical procedure based on equation (8.3). The above procedures should be possible using an on-line computer with memory access to the detector outputs without requiring excessively long imaging times, but we will postpone until later papers more precise details of particular implementations.

Super-resolution gains consistent with the results of the analysis of this paper have recently been achieved by numerical simulation [27], and the method promises significant improvements for diffraction-limited instrumental systems.

Acknowledgement

La théorie familière du transfert d'information en imagerie en utilisant les fonctions sphéroïdales et leur spectre de valeurs propres est étendue pour permettre que les domaines objet et image diffèrent. La théorie appropriée devient une des fonctions singulières et des valeurs singulières et on donne, dans cet article, une description de l'imagerie cohérente en ces termes. La super-résolution au sens de l'amélioration sur les critères antérieurs en présence de

bruit peut alors être réalisée, particulièrement aux très bas nombres de Shannon, en utilisant l'image physique continue; on donne des évaluations quantitatives de telles améliorations pour les cas de pupilles rectilignes, carrées et circulaires.

On montre aussi que la théorie fournit une épreuve efficace du théorème disant que le nombre de degrés de liberté d'un système d'imagerie isoplanétique cohérent n'est pas affecté par des aberrations de phase dans la pupille.

Des applications de ces résultats en microscopie sont donnés et une méthode pratique de mise en oeuvre est proposée; elle est basée sur la généralisation des techniques d'inversion numérique récemment développées dans le domaine de la diffusion laser.

Die bekannte Abbildungstheorie mit Sphäroidfunktionen und deren Eigenwertspektrum wird auf den Fall ausgedehnt, daß sich Objekt- und Bildbereich unterscheiden. Die hierfür geeignete Theorie wird zu einer Theorie singulärer Funktionen und Werte und wir geben in der vorliegenden Arbeit eine Beschreibung der kohärenten Abbildung mit diesen Ausdrücken. Überauflösung im Sinne einer Verbesserung bezüglich vorgegebener Kriterien kann bei Vorliegen von Rauschen insbesondere bei sehr kleinen Shannon-Zahlen erzielt werden, wenn das physikalisch fortgesetzte Bild benutzt wird und wir geben quantitative Abschätzungen solcher Verbesserungen für die lineare, quadratische und kreisförmige Pupille.

Ferner wird gezeigt, daß diese Theorie auch eine brauchbare Bestätigung des Theorems liefert, wonach die Anzahl der Freiheitsgrade eines kohärenten isoplanatischen Abbildungssystems von Phasenaberrationen in der Pupille unbeeinträchtigt bleibt.

Anwendungen dieser Ergebnisse in der Mikroskpie werden skizziert und eine praktische Methode zur Implementierung wird vorgeschlagen, die auf einer Verallgemeinerung numerischer Integrationstechniken beruht, wie sie kürzlich in Bereich der Laserlichtstreuung entwickelt worden sind.

References

[1] TORALDO DI FRANCIA, G., 1969, *J. opt. Soc. Am.*, **59**, 799.

[2] FRIEDEN, B. R., 1971, *Progress in Optics*, Vol. IX, edited by E. Wolf (Amsterdam: North-Holland), p. 311.

[3] HADAMARD, J., 1923, *Lectures on the Cauchy Problem in Linear Partial Differential Equations* (Yale University Press).

[4] WOLTER, H., 1961, *Progress in Optics*, Vol. I, edited by E. Wolf (Amsterdam: North-Holland), p. 155.

[5] HARRIS, J. L., 1964, *J. opt. Soc. Am.*, **54**, 931.

[6] BERTERO, M., DE, MOL, C., and VIANO, G. A., 1980, *Inverse Scattering Problems in Optics*, edited by H. P. Baltes, Topics in Current Physics Vol. 20 (Berlin, Heidelberg, New York: Springer-Verlag), p. 161.

[7] LO, Y. T., 1961, *J. appl. Phys.*, **32**, 2052.

[8] McCUTCHEN, C. W., 1967, *J. opt. Soc. Am.*, **57**, 1190.

[9] PASK, C., 1976, *J. opt. Soc. Am.*, **66**, 68.

[10] TIKHONOV, A. N., and ARSENIN, V. Y., 1977, *Solution of Ill-Posed Problems*, translation edited by F. John (New York: Wiston–Wiley).

[11] BIRAUD, Y., 1969, *Astron. Astrophys.*, **1**, 124.

[12] FRIEDEN, B. R., 1975, *Picture Processing and Digital Filtering*, edited by T. S. Huang, Topics in Applied Physics Vol. 6 (Berlin, Heidelberg, New York: Springer-Verlag), p. 177.

[13] RUSHFORTH, C. K., and HARRIS, R. W., 1968, *J. opt. Soc. Am.*, **58**, 539.

[14] GOODMAN, J. W., 1970, *Progress in Optics*, Vol. VIII, edited by E. Wolf (Amsterdam: North-Holland), p. 1.

[15] GERCHBERG, R. W., 1974, *Optica Acta*, **21**, 709.

[16] MILLER, G. F., 1974, *Numerical Solution of Integral Equations*, edited by L. M. Delves and J. Walsh (Oxford: Clarendon Press), p. 175.

[17] SLEPIAN, D., and POLLAK, H. O., 1961, *Bell Syst. tech. J.*, **40**, 43.

[18] RINO, C. L., 1969, *J. opt. Soc. Am.*, **59**, 547.

[19] DE SANTIS, P., and PALMA, C., 1976, *Optica Acta*, **23**, 743.
[20] GOODMAN, J. W., 1968, *Introduction to Fourier Optics* (New York: McGraw-Hill).
[21] SLEPIAN, D., 1964, *Bell Syst. tech. J.*, **43**, 3009.
[22] SHEPPARD, C. J. R., and WILSON, T., 1980, *Optik*, **55**, 331.
[23] JAKEMAN, E., PIKE, E. R., and SWAIN, S., 1971, *J. Phys.* A, **4**, 517.
[24] WALKER, J. G., 1981, *Optica Acta*, **38**, 735.
[25] MCWHIRTER, J. G., 1980, *Optica Acta*, **27**, 83.
[26] OSTROWSKI, N., SORNETTE, D., PARKER, P., and PIKE, E. R., 1981, *Optica Acta*, **28**, 1059.
[27] BERTERO, M., PARKER, P., and PIKE, E. R., 1982.